Coronal Mass Ejection of 28 June 2000: Coupling of the CME Evolution and the Flare Energy Release

D.Maričić[1], D.Roša[1], B. Vršnak[2]

[1]Astronomical Observatory Zagreb, Zagreb, Croatia, darije.maricic@zg.htnet.hr, drosa@hpd.botanic.hr
[2]Hvar Observatory, Faculty of Geodesy, Zagreb, Croatia, bvrsnak@geodet.geof.hr

We study the initiation and development of the limb Coronal Mass Ejection (CME) of 28 Jun 2000, utilizing observations from Mauna Loa Solar Observatory (MLSO), the Solar and Heliospheric Observatory (SOHO), the Geostationary Operational Environmental Satellite (GOES) and Yohkoh. Also, we analyze the relation between dynamics of the Coronal Mass Ejection (CME) and the energy release in the associated flare.

The basic structure of the CME (prominence imbedded in bright coronal arcade) is clearly recognizable already in the low corona during the pre-eruption phase of slow rise. This provided measurements of kinematics of various features from the very beginning of the eruption up to the post-acceleration phase which was followed up to 32 solar radii. Such events are observed only occasionally, and are of great importance for the comprehension of the nature of forces driving CMEs. The acceleration maximum was attained at the radial distance of 1.45 solar radii from the Sun's center and ceased beyond 4 solar radii. The acceleration phase was synchronized with the impulsive phase of the associated two-ribbon flare.

Observations provide clear evidence that the CME eruption caused a global restructuring of the magnetic field in the outer and inner corona.

Introduction

Coronal Mass Ejections (CMEs) are eruptions of large-scale coronal magnetic field structures. They are solar phenomena during which 10^{11} – 10^{13} kg of atmospheric magnetoplasma is launched into interplanetary space at speeds ranging from several tens kms^{-1}, up to 2000 kms^{-1}. CMEs often expose a three-part structure: the prominence, the cavity and the leading edge, as in [1, 2, 4, 7]. In this respect, observations in soft X-rays and solar eclipse observation have revealed an analogues quiescent prominence/corona structure (the prominence is usually found in a coronal void nested in the helmet streamer), indicating that the basic CME morphology has its roots in the pre-eruption magnetic field configuration. Observations of CMEs show several evolutionary phases (see e.g., [5, 8, 10, 13]):

- Slow rising motion (quasi-stationary evolution of the pre-eruptive structure through a series of equilibrium states).
- The acceleration phase most often starts by an exponential-like development.
- Post-acceleration phase, CMEs showing approxi-mately constant velocity.

The association of CMEs and eruptive prominences provides important information regarding the process of initiation.

One of the fundamental problems of these most spectacular events is that we still do not understand the physics of initiation, trigger mechanism, formation phase and the nature of forces driving the CMEs. What are the processes by which CMEs are accelerated? Most probably, the mechanisms of eruption include catastrophic loss of equilibrium and some large-scale instabilities such as the MHD kink instability. It has been shown recently that process of eruption can be significantly affected by the process of reconnection below the rising flux-rope [3]. Our results are consistent with this hypothesis, since the acceleration of the CME was strongly correlated with the energy release in the associated two-ribbon flare which is governed by the reconnection below the erupting flux rope [11].

In this paper, we present a detailed analysis of the kinematics of basic morphological features of the fast limb CME of 28 June 2000, from the pre-acceleration phase up to 30 solar radii. In addition, we analyze the relationship between the CME dynamics and the energy release in the associated flare.

The data set

The eruption 28 Jun 2000 was recorded by a number of ground-based and space-borne instruments. The FeXII 195Å images of the Extreme Ultraviolet Imaging Telescope (EIT) on board the Solar and Heliospheric Observatory (SOHO) are employed to measure the height of the EUV arcade overlying the prominence. The HeI images recorded at the Mauna Loa Solar Observatory/Heigh Altitude Observatory (MLSO/HAO) are used to follow the kinematics of the upper edge of the prominence. Data from the Soft X-Ray Telescope (SXT) aboard the Yohkoh satellite are utilized to inspect the morphology of the event in the pre-eruption phase. The soft X-ray (SXR) flux measurements in the 1-8 Å and 0.5-4 Å channels of the Geostationary Operational Environmental Satellite (GOES) are used to get information on the energy release in the associated flare.

The eruptive prominence is traced through the inner corona utilizing the Hα and white-light images of the Mauna Loa Solar Observatory (MLSO), gained by Polarimetar for Inner Coronal Studies (PICS) and the MK-IV K-coronameter, respectively. Also, white-light data acquired by the Large Angle and Spectrometric Coronagraphs (LASCO) on board SOHO, are used to follow the tree-part structure of the CME from the inner corona to the interplanetary space.

General description of the 28 Jun 2000 event

The event took place at the west limb, starting at the position angle PA≈290°. It was associated with the eruptive prominence observed in Hα and HeI. In late phase of the event EIT images expose a huge system of growing post flare loops, disclosing a long-duration energy release, consistent with the GOES measurements which show a relatively gradual SXR burst. The EIT images reveal a coronal arch-like feature overlaying the prominence. It became visible in the EIT image 18:36 UT at a height of 1.26Rsun, showing a gradual outward expansion. Between the leading edge of the CME and the prominence a dark cavity developed. The initial rise of the arch, which later becomes the frontal rim of CME, was tracked in the EIT images. Its further kinematics was measured utilizing the MK-IV data, partly overlapping with the EIT field of view.

In MK-IV, C2, and C3 coronagraph images the CME exposes a clearly recognizable three-part structure. The frontal rim was nearly circular. The entire structure maintained its integrity while propagating through the MK-IV, C2 and C3 fields of view. In the pre-acceleration phase, the prominence did not show rotational motions and during the acceleration phase, the prominence axis became kinked (see the EIT, MK-IV and LASCO C2 images in Fig. 1).

The GOES soft X-ray flux measurements in the 1-8 Å and 0.5-4 Å channel show that the CME was associated with a gradual burst of the GOES class C6. The burst started with a

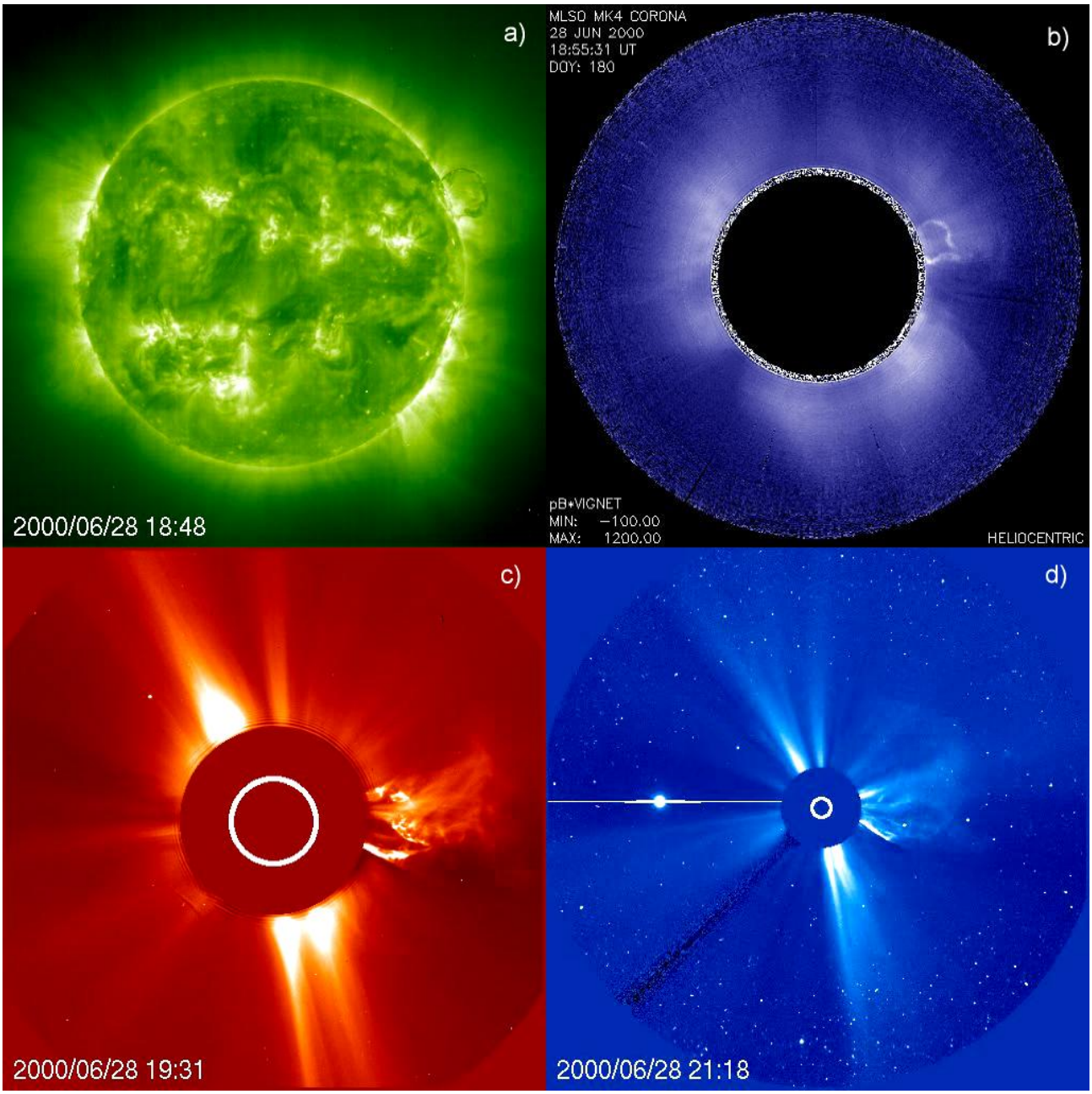

Fig. 1. Evolution of 28 Jun 2000 CME a) EIT FeXII 195 Å image, showing the prominence; b) MK-IV images taken at 18:55 UT; c) LASCO C2 images taken at 19:31 UT; d) LASCO C3 images taken at 21:18 UT. The MK-IV field of view R=1.08-2.85, partly overlaps with the EIT and LASCO C2 field of view.

precursor (≈ 18:35 – 18:45 UT), attained the maximum intensity at 19:10 UT, and than decayed in about 2 h.

Kinematics of the CME

The analysis of the kinematics is focused on the distance-time measurements of the leading edge of the CME and the top of the eruptive prominence. The kinematics of the frontal edge of CME, and the top of the prominence is traced by measuring the distance from the solar center, r. The $r(t)$ data measured by different instrument were joined and smoothed (for details of the procedure see [5]). To get a more reliable smooth trough the raw data we limited the smoothing intervals to specific phases of the eruption. In particular, we divided the eruption in the pre-acceleration phase, the main acceleration phase, and the late phase. From the smoothed data we evaluated the velocities by taking two successive smoothed data points [5]:

$$v(t_{vi}) = (r(t_{i+1}) - r(t_i))/(t_{i+1} - t_i), \qquad (1)$$

where $r(t_i)$ is the height at time t_i and $t_{vi} = (t_{i+1}+t_i)/2$.

Furthermore, in the following step we have estimated the acceleration by taking two successive velocity data points, by applying:

$$a(t_{ai}) = (v(t_{vi+1})-v(t_{vi}))/(t_{vi+1}-t_{vi}), \qquad (2)$$

where $t_{ai} = (t_{vi+1}+t_{vi})/2$.

In Fig. 2a we display the raw data, covering a part of pre-acceleration phase and main acceleration phase for both CME components. The velocity-time profiles of the leading edge and the prominence are shown in Fig. 2b, whereas the acceleration-time is presented in Fig. 2c. In Fig. 2d we present the distance between leading edge and prominence $d = r_{\text{leading edge}} - r_{\text{prominence}}$, where $r_{\text{leading edge}}$ and $r_{\text{prominece}}$ are the heliocentric distances of the top of the leading edge and the top of the prominence, respectively.

The leading edge achieved the acceleration maximum of $a_{max} \approx 1850 \pm 150$ ms^{-2} at heliocentric distance of 1.45 solar radii around 18:50 UT. The prominence attained $a_{max} \approx 520 \pm 50$ ms^{-2}, at heliocentric distance 1.35 solar radii around 18:55

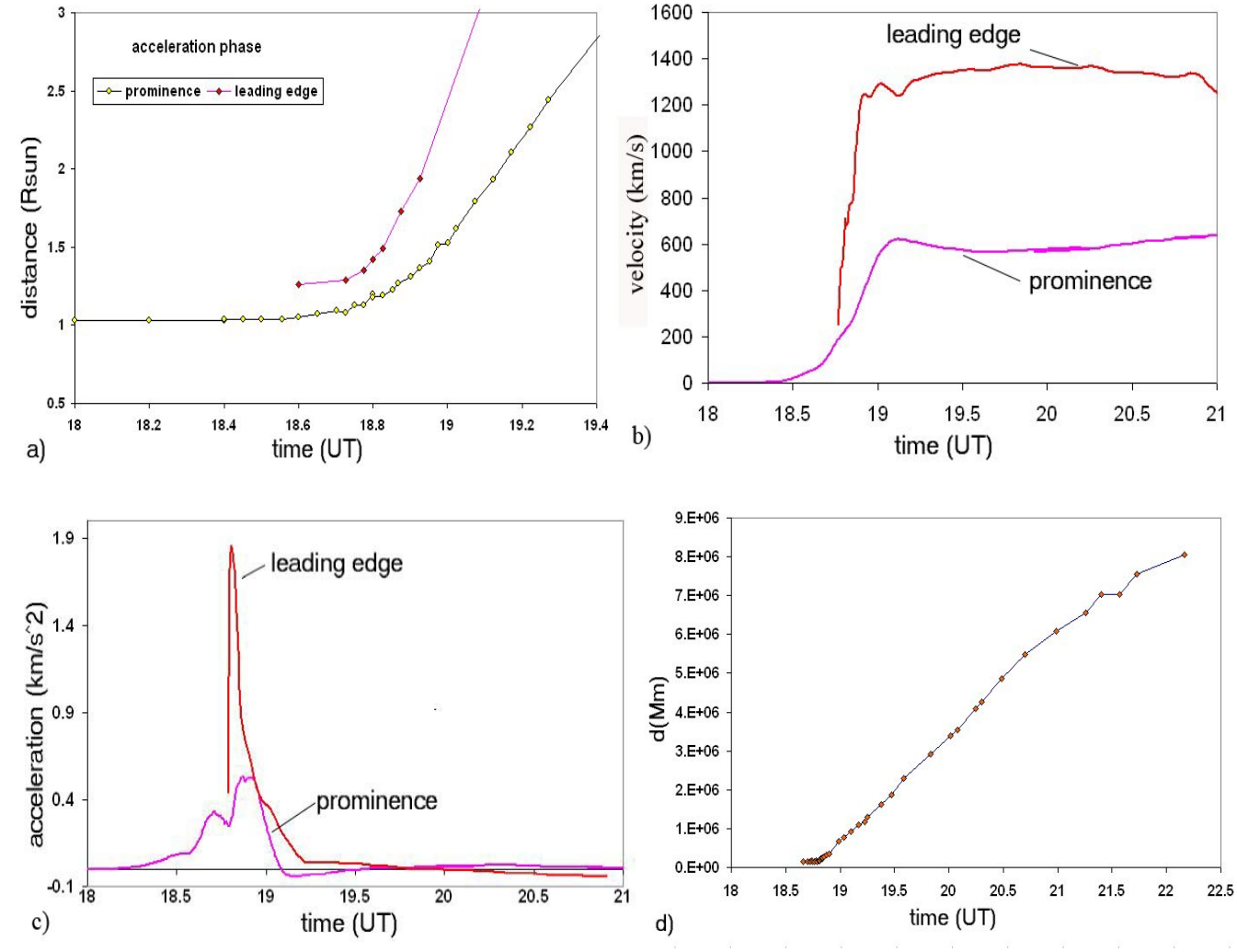

Fig. 2. Time profiles of the 28 Jun 2000 CME: a) radial distance; b) velocities derived from the smoothed data; c) acceleration; and d) the distance between leading edge and prominence (note a different scale of the x-axis). The raw data are depicted by diamonds representing the frontal edge, and the top of the prominence, respectively.

UT. The main acceleration phase of CME started at approximately 18:25 UT, and lasted for less than 50 min.

The acceleration decreased to 1/4 of the maximum acceleration at $R \approx 2.1$ solar radii for the leading edge and $R \approx$

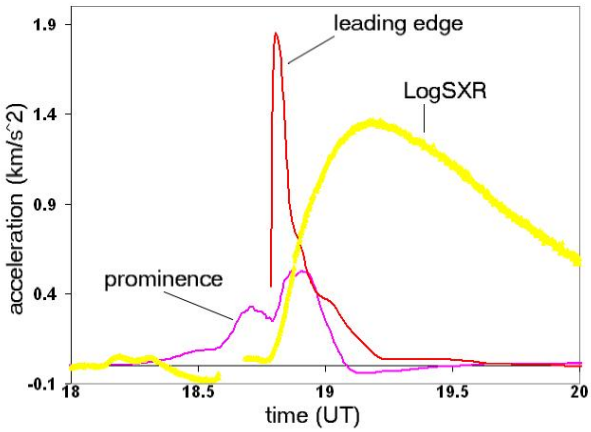

Fig. 3. The CME acceleration phase.

1.7 for the prominence. In the upper corona the velocity of both the leading edge and the prominence became roughly constant. The leading edge and the prominence attained velocities of about 1350 km/s and 620 km/s, respectively.

This is significantly faster than the ambient solar wind, which is flowing roughly at 100-200 km/s in C2 field of view and 200-300 km/s farther out, on average asymptotically increasing towards 400 km/s [6]. The leading edge was gradually decelerating in the C3 field of view, most likely due to the "aerodynamic" drag [9]. The denser, and more inert prominence decelerating latter then frontal rim.

In Fig. 3, the GOES 0.5-4Å SXR flux is compared with corresponding acceleration time-profiles of the leading edge of the CME and the prominence. The interval of the SXR burst growth, indicating the highest energy release rate in the flare, shows an almost perfect match with the CME acceleration phase (for similar events see [5, 8, 10, 12, 13]).

Discussion and Conclusion

The presented multi-wavelength analysis of the eruption shows that this event could be considered as a typical example of an impulsive CME [13]. We summarize the results as follows:

- The CME exhibits the classical three-part structure
- The CME is seen to ascend for one hour with low speed of less than 10 km/s in the lower corona.
- A bright loop-shaped structure, corresponding to the frontal rim of the CME, is observed already in the pre-acceleration phase at the radial distance of 1.26 solar radii. The speed of 1400 kms^{-1} was attained in less than 1/2 hour.
- The peak acceleration amounts to 1.9 kms^{-2}.
- The speed versus distance plot is similar for both the leading edge of the CME and the eruptive prominence. This suggests that the same mechanism drives both the leading edge of the CME and the prominence.
- The acceleration phase is simultaneous with the growth of the associated SXR flare.

Acknowledgements

We would like to thank the GOES, MLSO, SOHO, and Yohkoh teams for developing and operating the instruments and we are grateful for their open data policy.

REFERENCES

[1] J. Chen, *Astrophys. J.*, Vol. 338, 1989, p.453.
[2] R. Fisher, A.I. Poland, *Astrophys. J.*, Vol. 246, 1981, p. 1004.
[3] J. Lin, J.C. Raymond, A.A. van Ballegooijen, *Astrophys. J.*, Vol. 602, 2004, p. 422.
[4] B.C. Low, R.H. Munro, R.R. Fisher, *Astrophys. J.*, Vol. 254, 1982, p. 335.
[5] D. Maričić et al., *Solar Phys*., Vol. 225, 2004, p. 337.
[6] N. R. Jr. Sheeley, et al., *Astrophys. J.*, Vol. 484, 1997, p. 472.
[7] N. Srivastava, et al., *Astrophys. J.*, Vol. 534, 2000, p. 468.
[8] B. Vršnak, *J. Geophys. Res*., Vol. 106, 2001, p. 25249.
[9] B. Vršnak, *Solar Phys*., Vol. 202, 2001, p. 173.
[10] B. Vršnak, et al., *Solar Phys*., Vol. 225, 2004, p. 355.
[11] B.E. Wood, et al., *Astrophys. J.*, Vol. 512, 1999, p. 484.
[12] J. Zhang, et al., *Astrophys. J.*, Vol. 559, 2001, p.452.
[13] J. Zhang, et al., *Astrophys. J.*, Vol. 604, 2004, p. 420.